Dominance of the Breit interaction in the cross section and circular polarization of x-ray radiation following longitudinally-polarized-electron-impact excitation of highly charged ions

Zhan-Bin Chen, Chen-Zhong Dong,* and Jun Jiang

Key Laboratory of Atomic and Molecular Physics and Functional Materials of Gansu Province, College of Physics and Electronic Engineering, Northwest Normal University, Lanzhou 730070, People's Republic of China

(Received 6 July 2014; published 25 August 2014)

Longitudinally-polarized-electron-impact excitation cross sections from the ground state to the individual magnetic sublevels of the excited state $1s2s^22p_{3/2}(J=2)$ of highly charged Be-like ions are calculated using a fully relativistic distorted-wave method. The contributions of the Breit interaction to the cross sections and circular polarizations of the $1s2s^22p_{3/2}(J=2)\rightarrow 1s^22s^2(J=0)$ magnetic quadrupole ($M2$) line for selected Be-like Ag^{43+}, Ho^{63+}, and Bi^{79+} ions are investigated systematically. It is found that the Breit interaction has a large effect and makes the cross sections increase, especially to the $m_f=-1$ and -2 sublevels, the Breit interaction can modify the cross sections by several orders of magnitude. These dramatic influences also lead to a remarkable decrease in the circular polarization of subsequent x-ray radiation, the character of which becomes more and more evident with increasing incident energy and atomic number. And all these characteristics are very different from the conclusions for the linear polarization of radiation following the electron-impact process [S. Fritzsche, A. Surzhykov, and T. Stöhlker, Phys. Rev. Lett. **103**, 113001 (2009); Z. W. Wu, J. Jiang, and C. Z. Dong, Phys. Rev. A **84**, 032713 (2011)].

DOI: 10.1103/PhysRevA.90.022715 PACS number(s): 34.80.Dp, 34.80.Lx

I. INTRODUCTION

The polarization of x-ray line emission from highly charged ions undergoing collisions with an electron beam has been a topic of continuous fundamental interest for decades [1–26]. When compared to the conventional observable cross sections or rate coefficients, such polarization studies were found to be much more effective with regard to the details of the various effects and interactions and, in fact, helped provide new insight into the electron-electron and electron-photon interactions in the presence of strong Coulomb fields.

Until now, however, most theoretical studies on the x-ray emission have assumed that the incident electron beam is unpolarized. As a consequence, the excitation cross sections needed in investigating the characteristics of the emitted radiation were presented for the different $|M_J|$ magnetic sublevels because there is no population selection between the sublevels M_J and $-M_J$. This implies that only linearly polarized radiation was considered [27]. As is well known, the excitation of ions by a polarized electron beam will lead to an orientation of the excited level in general; i.e., the magnetic sublevels M_J and $-M_J$ are differently populated. The radiation subsequently emitted in the decay of these oriented levels is circularly polarized. Early work on the circular polarization of the x-ray line emission was performed by Inal and coworkers [27–29]. In these investigations, the relativistic effects and inner-shell ionization effects were studied for the decay of He-like Fe^{24+} ions following the excitation process. Hereby, the main emphasis was only placed on relatively low-Z systems; there have been no previous theoretical calculations for the cross sections and circular polarization properties in the high-Z domain. Recently, some works have included the experimental verification of the importance of the Breit interaction for few-electron ions [30–34] and the successful reinterpretation of the linear polarization of x-ray emission in high-Z ions. For example, Bostock *et al.* [35] have calculated the degree of linear polarization of the Lyman-α_1 line for H-like ions excited by the electron-impact excitation process using the relativistic convergent close-coupling method. They found that an account of Breit relativistic corrections is important to resolve the discrepancy between experimental and theoretical calculations. Fritzsche *et al.* [33] have calculated the linear polarization of Be-like ions following the dielectronic recombination process; they found that the Breit interaction strongly dominates the Coulomb repulsion and leads to a qualitative change in linear polarization. This predicted phenomenon has recently been observed and confirmed experimentally [31]. Wu *et al.* [36] have analyzed the influence of the Breit interaction on the linear polarization following electron-impact excitation of Be-like ions. When compared with the dielectronic recombination process, a quite different behavior is found for the polarization of the same line. Therefore, some similar effects of the Breit interaction should also be expected for the cross sections and circular polarizations of x-ray radiation following impact excitation by the longitudinally polarized electron.

In the present work, the computationally fast and accurate fully relativistic distorted-wave (RDW) program REIE06 [25,36–38] is designed to calculate the impact excitation cross sections by the longitudinally polarized electron. As an example, the $1s^22s^2(J=0)\rightarrow 1s2s^22p_{3/2}(J=2)$ excitations of different charged Be-like ions Ag^{43+}, Ho^{63+}, and Bi^{79+} are studied systematically. Also, the influences of Breit interaction on the excitation cross sections and the degree of circular polarizations of subsequent x-ray radiation are discussed in detail. The paper is organized as follows. In Sec. II, we first provide a short description of the theoretical method and computational procedure. In Sec. III, the influences of the Breit interaction on the magnetic sublevel cross sections and the degree of circular polarizations of the corresponding line are discussed. Finally, some brief conclusions are given in Sec. IV.

*dongcz@nwnu.edu.cn

II. THEORETICAL METHOD

In the present work, target state wave functions are generated with the use of the atomic structure package GRASP92 [39] based on the multiconfiguration Dirac-Fock method, and the continuum electron wave functions are produced by the component COWF of the RATIP package [40] by solving the coupled Dirac equation in which the exchange effect between the bound and continuum electrons is considered. In this method, the z axis is chosen along the motion of the incident electron, and then the z component of the incident electron orbital angular momentum is zero, namely, $m_{l_i} = 0$. In this case, the longitudinally polarized electron-impact excitation cross section of the target ion from the initial state $\beta_i J_i M_i$ to the final state $\beta_f J_f M_f$ can be given by improving the formula [27–29]

$$\begin{aligned}
\sigma_{\varepsilon_i}(\beta_i J_i M_i - \beta_f J_f M_f) &= \frac{2\pi a_0^2}{k_i^2} \times \sum_{l_i,l_i',j_i,j_i',m_{s_i},l_f,j_f,m_f} \\
&\times \sum_{J,J',M} (i)^{l_i - l_{i'}} [(2l_i+1)(2l_i'+1)]^{1/2} \\
&\times \exp\left[i\left(\delta_{\kappa_i} - \delta_{\kappa_{i'}}\right)\right] C\left(l_i \frac{1}{2} m_{l_i} m_{s_i}; j_i m_i\right) \\
&\times C\left(l_i' \frac{1}{2} m_{l_i'} m_{s_i}; j_i' m_i\right) C(J_i j_i M_i m_i; JM) \\
&\times C(J_i j_i' M_i m_i; J'M) C(J_f j_f M_f m_f; JM) \\
&\times C(J_f j_f M_f m_f; J'M) R(\gamma_i, \gamma_f) R(\gamma_i', \gamma_f'),
\end{aligned} \tag{1}$$

where the subscripts i and f refer to the initial and final states, respectively; ε_i is the incident energy in Rydberg units; a_0 is the Bohr radius; C's are Clebsch-Gordan coefficients; R's are the collision matrix elements; $\gamma_i = \varepsilon_i l_i j_i \beta_i J_i JM$ and $\gamma_f = \varepsilon_f l_f j_f \beta_f J_f JM$, where J and M are the quantum numbers corresponding to the total angular momentum of the impact system, target ion plus free electron, and its z component, respectively; β represents all additional quantum numbers required to specify the initial and final states of the target ion in addition to its total angular momentum J and z component M; $m_{s_i}, l_i, j_i, m_{l_i}$, and m_i are the spin, orbital angular momentum, total angular momentum, and its z component quantum numbers, respectively, for the incident electron e_i; δ_{κ_i} is the phase factor for the continuum electron; κ is the relativistic quantum number, which is related to the orbital and total angular momentum l and j; k_i is the relativistic wave number of the incident electron, given by

$$k_i^2 = \varepsilon_i \left(1 + \frac{\alpha^2 \varepsilon_i}{4}\right); \tag{2}$$

and α is the fine-structure constant. It turns out that the $R(\gamma_i, \gamma_f)$ are independent of M,

$$R(\gamma_i, \gamma_f) = \left\langle \Psi_{\gamma_f} \right| \sum_{p,q,p<q}^{\mathrm{N+1}} (V_{\mathrm{Coul}} + V_{\mathrm{Breit}}) \left| \Psi_{\gamma_i} \right\rangle, \tag{3}$$

where V_{Coul} is the Coulomb operator, and V_{Breit} is the Breit operator, which can be given by [39]

$$\begin{aligned}
V_{\mathrm{Breit}} = &-\frac{\alpha_p \alpha_q}{r_{pq}} \cos(\omega_{pq} r_{pq}) \\
&+ (\alpha_p \nabla_p)(\alpha_q \nabla_q) \frac{\cos(\omega_{pq} r_{pq}) - 1}{\omega_{pq}^2 r_{pq}},
\end{aligned} \tag{4}$$

where α_p and α_q are the Dirac matrices and ω_{pq} is the angular frequency of the exchanged virtual photon. Ψ_{γ_i} and Ψ_{γ_f} are the antisymmetric $(N+1)$-electron wave functions for the initial and final states of the impact systems, respectively, which can be written as [25]

$$\begin{aligned}
\Psi_{\gamma_t} = &\frac{1}{(N+1)^{1/2}} \sum_{p=1}^{N+1} (-1)^{N+1-p} \sum_{M_t, m} C(J_t j M_t m; JM) \\
&\times \Phi_{\beta_t J_t}\left(x_p^{-1}\right) u_{\kappa m \varepsilon}(x_p),
\end{aligned} \tag{5}$$

where $(t = i, f)$; $\Phi_{\beta_t J_t}$ are the target-ion wave functions; x_p designates the space and spin coordinates for electron p; x_p^{-1} are the space and spin coordinates of all the N electrons other than p; and $u_{\kappa m \varepsilon}$ is the relativistic distorted-wave Dirac spinor for a continuum electron. The continuum orbitals with given electron energy are solutions of the Dirac-Fock equations, in which the direct and exchange potentials are considered.

The degree of circular polarization of radiation is defined as [27]

$$P_c = \frac{I_{\sigma^+} - I_{\sigma^-}}{I_{\sigma^+} + I_{\sigma^-}}, \tag{6}$$

where I_{σ^+} and I_{σ^-} are the intensities of left- and right-handed circularly polarized radiation, respectively. If we assume target ions devoid of hyperfine interactions and an incident electron beam that is completely longitudinally polarized, the polarization P_c observed in a direction along that of the electron beam is expressed in terms of the populations.

For the radiation from the $J = 2$ or 1 line to the $J = 0$ line, the circular polarization is given by [27,28]

$$P_c = \frac{\sigma_1 - \sigma_{-1}}{\sigma_1 + \sigma_{-1}}, \tag{7}$$

where σ_1 and σ_{-1} are the longitudinally polarized electron-impact excitation cross sections from the ground state to the magnetic sublevels $m_f = 1$ and -1 of the excited state, respectively.

III. RESULTS AND DISCUSSIONS

A. Comparisons of collision strength and circular polarization

As a check on our numerical methods, in Table I, the calculated collision strengths and circular polarizations with and without Breit interaction for longitudinally polarized electron excitation from the ground level to the $1s2p$ levels of He-like Fe^{24+} ions are listed, along with the existing theoretical values. It is found that the agreement with the different calculations is good in general for both the collision strengths and circular polarizations. For example, for the $1s^2(J=0) \rightarrow 1s2p_{1/2}(J=1)$ excitation, the present collision strengths without Breit interaction are 8.27×10^{-5}, 3.80×10^{-4}, and 2.87×10^{-4} for $m_f = -1$, 0, and 1 magnetic sublevels,

TABLE I. Comparison of the collision strengths and circular polarizations for excitation from the ground level to the different magnetic sublevels of the $1s2p$ levels for He-like Fe^{24+} ions by a longitudinally polarized electron. The rows labeled by NB and B stand for the values with only the Coulomb interaction included and the Coulomb plus Breit interaction included, respectively. The incident electron energy is 1200 Ry. R[n] means $R\times10^n$.

		Collision strength				Circular polarization	
Excited state	m_f	NB (others)	NB (ours)	B (others)	B (ours)	NB (others)	NB (ours)
$1s2p_{1/2}(J=0)$	0	5.17 (−5)[a]	5.27 (−5)	4.69 (−5)[a]	4.76 (−5)		
$1s2p_{3/2}(J=2)$	−2	3.63 (−9),[a] 3.60 (−9)[b]	4.02 (−9)	1.82 (−7)[a]	1.86 (−7)	0.822[b]	0.821
	−1	1.08 (−5),[a] 1.08 (−5)[b]	1.14 (−5)	1.52 (−5)[a]	1.59 (−5)		
	0	7.35 (−5),[a] 7.33 (−5)[b]	7.75 (−5)	8.19 (−5)[a]	8.36 (−5)		
	1	1.10 (−4),[a] 1.10 (−4)[b]	1.16 (−4)	1.10 (−4)[a]	1.15 (−4)		
	2	4.23 (−5),[a] 4.21 (−5)[b]	4.49 (−5)	4.44 (−5)[a]	4.74 (−5)		
$1s2p_{1/2}(J=1)$	−1	8.20 (−5)[b]	8.27 (−5)		8.98 (−5)	0.551[b]	0.553
	0	3.78 (−4)[b]	3.80 (−4)		3.58 (−4)		
	1	2.83 (−4)[b]	2.87 (−4)		3.21 (−4)		
$1s2p_{3/2}(J=1)$	−1	1.33 (−3)[b]	1.39 (−3)		1.41 (−3)	−0.310[b]	−0.331
	0	3.82 (−3)[b]	3.94 (−3)		3.75 (−3)		
	−1	1.25 (−3)[b]	1.30 (−3)		1.36 (−3)		

[a]See Ref. [29].
[b]See Ref. [27].

respectively. Compared with the theoretical values 8.20×10^{-5}, 3.78×10^{-4}, and 2.83×10^{-4}, an agreement of less than 3% is quoted for the differences between the results in Ref. [27] and the present calculated collision strengths. Moreover, the present circular polarization 0.553 is also in very good agreement with the result 0.551 calculated by Inal *et al.* [27].

B. The influence of Breit interaction on the excitation energies

After checking the method, we now turn to discuss effects of the Breit interaction on Be-like ions. To obtain accurate target state wave functions, in the calculations of wave functions and energy levels for the initial and final states, we consider the configurations $1s^22s^2$, $1s2s^22p$, and $1s^22p^2$, which give rise to a total of ten levels. The contributions from the quantum electrodynamics corrections are taken into account. In order to emphasize the contributions of the Breit interaction, we display two kinds of results with and without the Breit interaction included, respectively. For the only Coulomb calculations (labeled by NB), we use the Coulomb excitation energies and the Coulomb operator for the electron-impact matrix elements. Also, for the Coulomb plus Breit calculations (label by B), the Breit interaction is included in the calculations of the excitation energies and the electron-impact matrix elements. In Table II, the calculated excitation energies from the ground state $1s^22s^2(J=0)$ to the $1s2s^22p$ levels of highly charged Be-like ions are listed. It can been found that the present results are in very good agreement with others' theoretical results. Taking the $1s^22s^2(J=0)\rightarrow1s2s^22p_{3/2}(J=2)$ excitation of Fe^{22+} ions, for example, the present excitation energies with and without Breit interaction are 6612 and 6618 eV, respectively. Compared with the theoretical result 6613 eV given by Safronova and Shlyaptseva [41], an agreement of $<0.08\%$ is quoted for the differences between the result in Ref. [41] and the present calculated energies. It can also be found that the Breit interaction has a lager effect and makes the excitation energy decrease, and these effects become more important with increasing atomic number. For the $1s^22s^2(J=0)\rightarrow1s2s^22p_{3/2}(J=2)$ excitation, the contributions of the Breit interaction to the excitation energy are about 0.21%, 0.26%, and 0.30% for highly charged Ag^{43+}, Ho^{63+}, and Bi^{79+} ions, respectively.

C. The influence of Breit interaction on the cross sections

Figures 1(a)–1(c) display the total cross sections from the ground state $1s^22s^2(J=0)$ to the excited state $1s2s^22p_{3/2}(J=2)$ for Be-like Ag^{43+}, Ho^{63+}, and Bi^{79+} ions as

TABLE II. Excitation energies (in eV) from the ground state $1s^22s^2$ $(J=0)$ to the $1s2s^22p$ levels of Be-like ions. The rows labeled by NB and B stand for the values with only the Coulomb interaction included and the Coulomb plus Breit interaction included, respectively. The two sets of results for Bi^{79+} ions pertain to the two kinds of theoretical calculations in Ref. [36].

Ion	Excited state	NB (ours)	B (ours)	Others
Fe^{22+}	$1s2s^22p_{1/2}(J=0)$	6610	6606	6598[a]
	$1s2s^22p_{1/2}(J=1)$	6614	6608	6600[a]
	$1s2s^22p_{3/2}(J=1)$	6635	6628	6630[a]
	$1s2s^22p_{3/2}(J=2)$	6618	6612	6613[a]
Ag^{43+}	$1s2s^22p_{1/2}(J=0)$	22 541	22 506	
	$1s2s^22p_{1/2}(J=1)$	22 546	22 505	
	$1s2s^22p_{3/2}(J=1)$	22 778	22 739	
	$1s2s^22p_{3/2}(J=2)$	22 777	22 729	
Ho^{63+}	$1s2s^22p_{1/2}(J=0)$	47 672	47 589	
	$1s2s^22p_{1/2}(J=1)$	47 691	47 566	
	$1s2s^22p_{3/2}(J=1)$	48 709	48 593	
	$1s2s^22p_{3/2}(J=2)$	48 672	48 547	
Bi^{79+}	$1s2s^22p_{1/2}(J=0)$	76 242	76 081	
	$1s2s^22p_{1/2}(J=1)$	76 267	76 015	76 267,[b] 76 015[b]
	$1s2s^22p_{3/2}(J=1)$	78 923	78 689	
	$1s2s^22p_{3/2}(J=2)$	78 879	78 639	

[a]See Ref. [41].
[b]See Ref. [36].

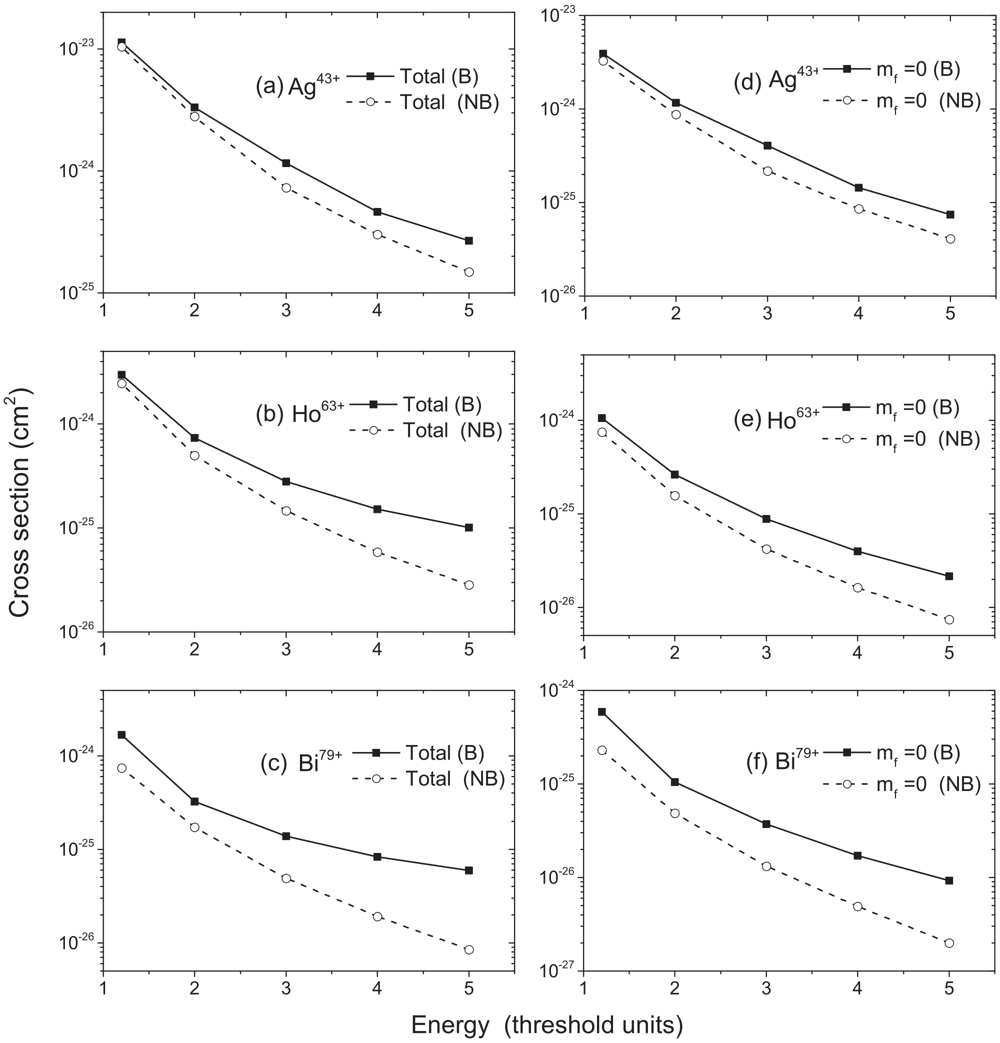

FIG. 1. Total and $m_f = 0$ magnetic sublevel cross sections for longitudinally-polarized-electron-impact excitation from the ground state $1s^2 2s^2 (J=0)$ to the excited state $1s2s^2 2p_{3/2} (J=2)$ for Be-like Ag^{43+}, Ho^{63+}, and Bi^{79+} ions as functions of incident polarized electron energy in threshold units. NB represents the values with inclusion of only the Coulomb interaction, and B represents the ones with the Breit interaction included.

a function of incident longitudinally polarized electron energy in threshold units. It is found that both total cross sections with and without the Breit interaction included decrease monotonically by the same pattern with increasing incident energy. They decrease rapidly near the threshold energy but decrease slowly within a higher-energy region. The Breit interaction makes the total cross sections increase at all given energies, and these effects become more and more evident with increasing incident energy and atomic number. The contributions of the Breit interaction to the total cross sections are about 9%, 21%, and 120% at 1.2 times the threshold energy and 80%, 256%, and 600% at five times the threshold energy for highly charged Ag^{43+}, Ho^{63+}, and Bi^{79+} ions, respectively.

In Figs. 1(d)–1(f), we show the $m_f = 0$ sublevel cross sections for Be-like Ag^{43+}, Ho^{63+}, and Bi^{79+} ions as a function of incident energy. As can be seen, the $m_f = 0$ sublevel cross sections follow a pattern very similar to the total cross sections. Also, the Breit interaction makes the cross sections increase, and these effects become more and more evident with increasing incident energy and atomic number.

Figures 2(a)–2(c) show the $m_f = \pm 2$ sublevel cross sections for excitation to the excited state $1s2s^2 2p_{3/2} (J = 2)$ for Be-like Ag^{43+}, Ho^{63+}, and Bi^{79+} ions as a function of incident longitudinally polarized electron energy. In the case of including only the Coulomb interaction, both the $m_f = 2$ and -2 sublevel cross sections decrease slowly with increasing incident energy. The cross sections for excitation to the sublevel $m_f = 2$ are significantly larger than these cross sections to the sublevel $m_f = -2$. The ratios of the σ_2/σ_{-2} are about 4.8×10^3, 1.7×10^3, and 9×10^2 at 1.2 times the threshold energy for the Be-like Ag^{43+}, Ho^{63+}, and Bi^{79+} ions, respectively. When the Breit interaction is taken into account, it is found that the Breit interaction makes the $m_f = \pm 2$ sublevel cross sections increase. The contributions of the Breit interaction to the $m_f = -2$ sublevel cross sections are very large, while those to the $m_f = 2$ sublevel cross sections are relatively small. Taking Be-like Bi^{79+} ions, for example, the Breit interaction can alter the cross sections by as much as a factor of 5×10^2 for excitation to the sublevel $m_f = -2$, while altering them by a factor of 7 for excitation to the sublevel

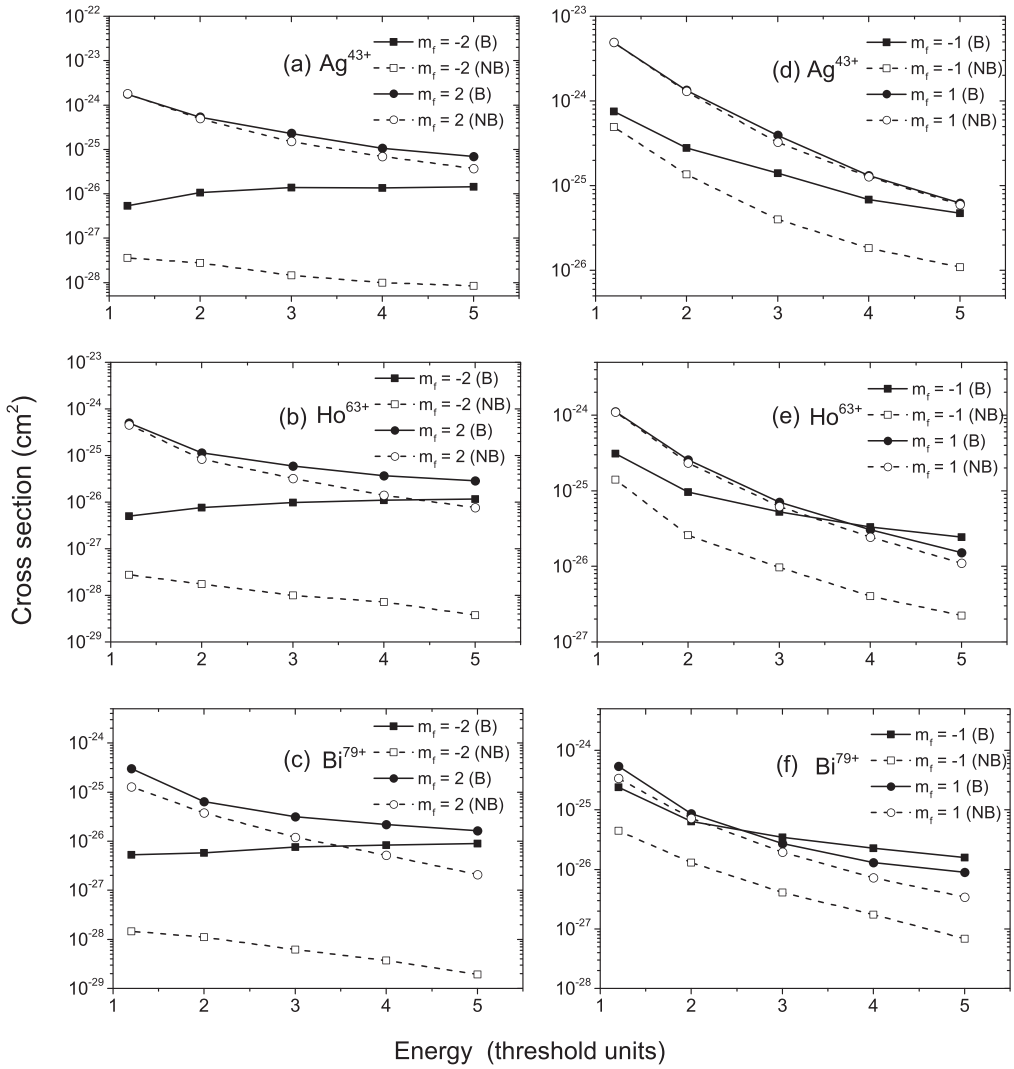

FIG. 2. Cross sections for longitudinally-polarized-electron-impact excitation from the ground state $1s^22s^2(J=0)$ to the specific magnetic sublevels $m_f = \pm 2$ and ± 1 of the excited state $1s2s^22p_{3/2}(J=2)$ for Be-like Ag^{43+}, Ho^{63+}, and Bi^{79+} ions as functions of incident polarized electron energy in threshold units. NB represents the values with inclusion of only the Coulomb interaction, and B represents the ones with the Breit interaction included.

$m_f = 2$ at five times the threshold energy. Moreover, for each particular ion, the Breit interaction becomes more and more apparent with increasing incident energy.

Figures 2(d)–2(f) show the $m_f = \pm 1$ sublevel cross sections of $1s2s^22p_{3/2}(J=2)$ for Be-like Ag^{43+}, Ho^{63+}, and Bi^{79+} ions as a function of incident polarized electron energy. In the case of including only the Coulomb interaction, both the $m_f = 1$ and -1 sublevel cross sections decrease slowly with increasing incident energy. The cross sections to the sublevel $m_f = 1$ are much larger than those to the sublevel $m_f = -1$. This character is quite similar with $m_f = \pm 2$ sublevels cross sections. The ratios of σ_1/σ_{-1} are about 10, 8, and 7.5 at 1.2 times the threshold energy for Be-like Ag^{43+}, Ho^{63+}, and Bi^{79+} ions, respectively. When the Breit interaction is taken into account, it is also found that the Breit interaction makes the cross sections for excitation to the sublevel $m_f = \pm 1$ increase. The contributions of the Breit interaction to the cross sections for excitation to the sublevel $m_f = -1$ are large, while those to the sublevel $m_f = 1$ are relatively small. For example, the Breit interaction altered the cross sections for excitation to the sublevel $m_f = -1$ by as much as a factor of 3.3, 10, and 22, while altering them by a factor of 0.03, 0.37, and 1.6 for excitation to sublevel $m_f = 1$ at about five times the threshold energy for Ag^{43+}, Ho^{63+}, and Bi^{79+} ions, respectively. Moreover, it is interesting to note that the two curves of cross sections for the sublevel $m_f = \pm 1$ with the Breit interaction included cross each other at about 3.6 and 2.2 times the threshold energy for Be-like Ho^{63+} and Bi^{79+} ions, respectively.

D. The influence of Breit interaction on the circular polarization

Figure 3 shows the circular polarization of the $1s2s^22p_{3/2}(J=2) \rightarrow 1s^22s^2(J=0)$ line of Be-like Ag^{43+}, Ho^{63+}, and Bi^{79+} ions as functions of incident polarized electron energy. In the case of including only the Coulomb interaction, the degree of circular polarization has a very large value and decreases very slowly with the increasing

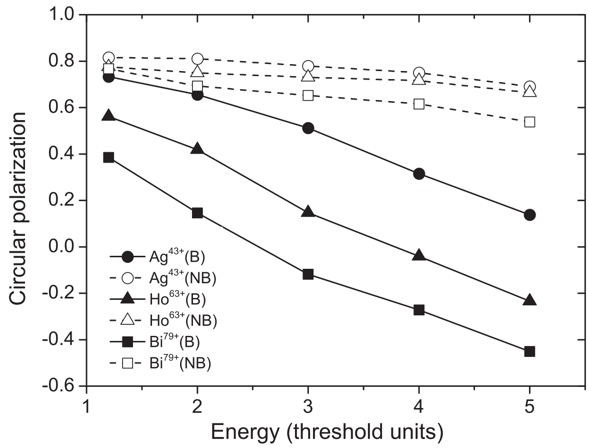

FIG. 3. The degree of circular polarization of the transition line $1s2s^22p_{3/2}(J=2)\rightarrow 1s^22s^2(J=0)$ for Be-like Ag^{43+}, Ho^{63+}, and Bi^{79+} ions as functions of incident polarized electron energy in threshold units. NB represents the values with inclusion of only the Coulomb interaction, and B represents the ones with the Breit interaction included.

incident energy. When the Breit interaction is taken into account, the circular polarization decreases rapidly for each ion with increasing energy. The Breit interaction decreases circular polarization from 0.79 to 0.22, 0.78 to −0.21, and 0.65 to −0.43 at five times the threshold energy for Be-like Ag^{43+}, Ho^{63+}, and Bi^{79+} ions, respectively. Moreover, the Breit interaction causes a change of the sign of the circular polarization for the Be-like Ho^{63+} and Bi^{79+} ions at about 4 and 2.2 times the threshold energy, respectively. The reason can be seen clearly from Figs. 2(e) and 2(f).

Finally, in Fig. 4, we display the degree of circular polarization with and without the Breit interaction included

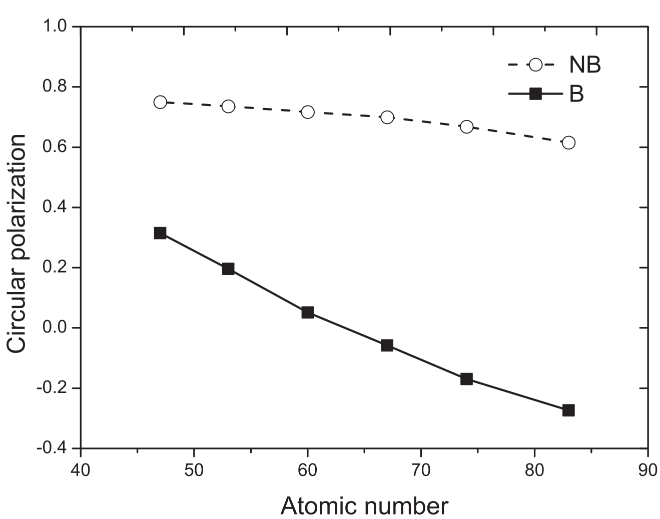

FIG. 4. The degree of circular polarization of the transition line $1s2s^22p_{3/2}(J=2)\rightarrow 1s^22s^2(J=0)$ for Be-like ions as functions of atomic number at incident polarized electron energy is four times the threshold energy. NB represents the values with inclusion of only the Coulomb interaction, and B represents the ones with the Breit interaction included.

as functions of atomic number at four times the threshold energy. It is obvious that the Breit interaction makes the degree of circular polarization decrease for all the Be-like ions. Also, the degree of circular polarization with only the Coulomb interaction included decreases very slowly as atomic number increases, while with inclusion of the Breit interaction it decreases rapidly. The Breit interaction decreases circular polarization from 0.73 to 0.32, 0.72 to −0.03, and 0.70 to −0.33 for Be-like Ag^{43+}, Ho^{63+}, and Bi^{79+} ions, respectively. These characteristics are different from the conclusions for the linear polarization [33,36] and the same line formed by the electron-impact excitation process [42], in which the Breit interaction makes the linear polarization increase, and the linear polarization with the Breit interaction included increases with increasing atomic number.

In the above sections, we have studied the circular polarization properties of x-ray photoemission following direct impact excitation. Admittedly, besides the direct impact excitation, some other effects such as the resonance impact excitation may greatly affect the magnetic sublevel cross sections and the circular polarizations of the corresponding lines for de-excitation processes in some cases. However, according to our estimates, in the present energy region, the resonance mainly comes from relatively high levels, whose corrections to the circular polarizations of the line of interest are relatively small. Therefore, these effects on the excitation and de-excitation processes are neglected in the present calculations.

IV. CONCLUSIONS

In summary, longitudinally polarized electron excitation cross sections and the degree of circular polarizations of subsequent x-ray emission of the $1s2s^22p_{3/2}(J=2)\rightarrow 1s^22s^2(J=0)$ line for highly charged Be-like Ag^{43+}, Ho^{63+}, and Bi^{79+} ions have been calculated using a fully RDW method. The influences of Breit interaction on the cross sections and the circular polarizations have been analyzed. For the excitation process, the Breit interaction makes both total and magnetic sublevel cross sections increase. The Breit interaction can modify the $m_f = -1$ and -2 sublevel cross sections by several orders of magnitude, the influences of which are much larger than the total and $m_f = 0$, 1, and 2 sublevel cross sections. For the de-excitation process, the Breit interaction makes the degree of circular polarization decrease, and the contributions of the Breit interaction to the degree of circular polarization becomes more and more evident with increasing incident polarized electron energy and atomic number. All these characteristics are very different from the conclusions for the linear polarization formed by the electron-impact process.

ACKNOWLEDGMENT

This work was supported by the National Natural Science Foundation of China (Grants No. 11274254, No. 11147018, and No. U1332206).

[1] J. R. Henderson, P. Beiersdorfer, C. L. Bennett, S. Chantrenne, D. A. Knapp, R. E. Marrs, M. B. Schneider, K. L. Wong, G. A. Doschek, J. F. Seely, C. M. Brown, R. E. LaVilla, J. Dubau, and M. A. Levine, Phys. Rev. Lett. **65**, 705 (1990).
[2] P. Beiersdorfer, D. A. Vogel, K. J. Reed, V. Decaux, J. H. Scofield, K. Widmann, G. Hölzer, E. Förster, O. Wehrhan, D. W. Savin, and L. Schweikhard, Phys. Rev. A **53**, 3974 (1996).
[3] E. Takács, E. S. Meyer, J. D. Gillaspy, J. R. Roberts, C. T. Chantler, L. T. Hudson, R. D. Deslattes, C. M. Brown, J. M. Laming, J. Dubau, and M. K. Inal, Phys. Rev. A **54**, 1342 (1996).
[4] A. S. Shlyaptseva, R. C. Mancini, P. Neill, and P. Beiersdorfer, Rev. Sci. Instrum. **68**, 1095 (1997).
[5] P. Beiersdorfer, J. C. López-Urrutia, V. Decaux, K. Widmann, and P. Neill, Rev. Sci. Instrum. **68**, 1073 (1997).
[6] Y. Itikawa, R. Srivastava, and K. Sakimoto, Phys. Rev. A **44**, 7195 (1991).
[7] M. K. Inal and J. Dubau, J. Phys. B **20**, 4221 (1987).
[8] M. K. Inal and J. Dubau, Phys. Rev. A **47**, 4794 (1993).
[9] P. Beiersdorfer, G. Brown, S. Utter, P. Neill, K. J. Reed, A. J. Smith, and R. S. Thoe, Phys. Rev. A **60**, 4156 (1999).
[10] F. Walden, H.-J. Kunze, A. Petoyan, A. Urnov, and J. Dubau, Phys. Rev. E **59**, 3562 (1999).
[11] N. Nakamura, D. Kato, N. Miura, T. Nakahara, and S. Ohtani, Phys. Rev. A **63**, 024501 (2001).
[12] D. L. Robbins, A. Ya. Faenov, T. A. Pikuz, H. Chen, P. Beiersdorfer, M. J. May, J. Dunn, K. J. Reed, and A. J. Smith, Phys. Rev. A **70**, 022715 (2004).
[13] D. L. Robbins, P. Beiersdorfer, A. Ya. Faenov, T. A. Pikuz, D. B. Thorn, H. Chen, K. J. Reed, A. J. Smith, K. R. Boyce, G. V. Brown, R. L. Kelley, C. A. Kilbourne, and F. S. Porter, Phys. Rev. A **74**, 022713 (2006).
[14] Y. M. Liu, S. Singha, T. E. Witt, Y. T. Cheng, and R. J. Gordon, Appl. Phys. Lett. **93**, 161502 (2008).
[15] K. J. Reed and M. H. Chen, Phys. Rev. A **48**, 3644 (1993).
[16] L. Sharma, A. Surzhykov, R. Srivastava, and S. Fritzsche, Phys. Rev. A **83**, 062701 (2011).
[17] P. Amaro, F. Fratini, S. Fritzsche, P. Indelicato, J. P. Santos, and A. Surzhykov, Phys. Rev. A **86**, 042509 (2012).
[18] C. J. Fontes, H. L. Zhang, and D. H. Sampson, Phys. Rev. A **59**, 295 (1999).
[19] M. K. Inal, A. Surzhykov, and S. Fritzsche, Phys. Rev. A **72**, 042720 (2005).
[20] T. Kai, R. Srivastava, and S. Nakazaki, Phys. Rev. A **70**, 062705 (2004).
[21] T. Kai, S. Nakazaki, and K. A. Berrington, Nucl. Instrum. Methods Phys. Res. B **235**, 249 (2005).
[22] T. Kai, S. Nakazaki, T. Kawamura, H. Nishimura, and K. Mima, Phys. Rev. A **75**, 012703 (2007).
[23] T. Kai, S. Nakazaki, T. Kawamura, H. Nishimura, and K. Mima, Phys. Rev. A **75**, 062710 (2007).
[24] Z. Q. Wu, Y. M. Li, B. Duan, J. Yan, and H. Zhang, Chin. Phys. Lett. **24**, 1560 (2007).
[25] J. Jiang, C. Z. Dong, L. Y. Xie, J. G. Wang, J. Yan, and S. Fritzsche, Chin. Phys. Lett. **24**, 691 (2007).
[26] M. H. Chen and J. H. Scofield, Phys. Rev. A **52**, 2057 (1995).
[27] M. K. Inal, H. L. Zhang, and D. H. Sampson, Phys. Rev. A **46**, 2449 (1992).
[28] M. K. Inal, D. H. Sampson, H. L. Zhang, and J. Dubau, Physica Scripta **55**, 170 (1997).
[29] M. K. Inal, H. L. Zhang, D. H. Sampson, and C. J. Fontes, Phys. Rev. A **65**, 032727 (2002).
[30] N. Nakamura, A. P. Kavanagh, H. Watanabe, H. A. Sakaue, Y. Li, D. Kato, F. J. Currell, and S. Ohtani, Phys. Rev. Lett. **100**, 073203 (2008).
[31] Z. Hu, X. Han, Y. Li, D. Kato, X. Tong, and N. Nakamura, Phys. Rev. Lett. **108**, 073002 (2012).
[32] A. Gumberidze, D. B. Thorn, C. J. Fontes, B. Najjari, H. L. Zhang, A. Surzhykov, A. Voitkiv, S. Fritzsche, D. Banas, H. Beyer, W. Chen, R. D. DuBois, S. Geyer, R. E. Grisenti, S. Hagmann, M. Hegewald, S. Hess, C. Kozhuharov, R. Martin, I. Orban, N. Petridis, R. Reuschl, A. Simon, U. Spillmann, M. Trassinelli, S. Trotsenko, G. Weber, D. F. A. Winters, N. Winters, D. Yu, and Th. Stöhlker, Phys. Rev. Lett. **110**, 213201 (2013).
[33] S. Fritzsche, A. Surzhykov, and T. Stöhlker, Phys. Rev. Lett. **103**, 113001 (2009).
[34] D. Bernhardt, C. Brandau, Z. Harman, C. Kozhuharov, A. Muller, W. Scheid, S. Schippers, E. W. Schmidt, D. Yu, A. N. Artemyev, I. I. Tupitsyn, S. Bohm, F. Bosch, F. J. Currell, B. Franzke, A. Gumberidze, J. Jacobi, P. H. Mokler, F. Nolden, U. Spillman, Z. Stachura, M. Steck, and T. Stöhlker, Phys. Rev. A **83**, 020701(R) (2011).
[35] C. J. Bostock, D. V. Fursa, and I. Bray, Phys. Rev. A **80**, 052708 (2009).
[36] Z. W. Wu, J. Jiang, and C. Z. Dong, Phys. Rev. A **84**, 032713 (2011).
[37] J. Jiang, C. Z. Dong, L. Y. Xie, and J. G. Wang, Phys. Rev. A **78**, 022709 (2008).
[38] Z. B. Chen, C. Z. Dong, L. Y. Xie, and J. Jiang, Phys. Rev. A **90**, 012703 (2014).
[39] F. A. Parpia, C. F. Fischer, and I. P. Grant, Comput. Phys. Commun. **94**, 249 (1996).
[40] S. Fritzsche, H. Aksela, C. Z. Dong, S. Heinäsmäki, and J. E. Sienkiewicz, Nucl. Instrum. Methods Phys. Res. B **205**, 93 (2003).
[41] U. I. Safronova and A. S. Shlyaptseva, Phys. Scripta **54**, 254 (1996).
[42] Y. L. Shi, C. Z. Dong, X. Y. Ma, Z. W. Wu, L. Y. Xie, and S. Fritzsche, Chin. Phys. Lett. **30**, 063401 (2013).